



## ELECTROCHEMICAL HYDROGEN PEROXIDE GENERATION AND REMOVAL OF MOXIFLOXACIN BY ELECTRO-FENTON PROCESS

Gökçe Didar DEĞERMENCİ<sup>1\*</sup>, Nejdet DEĞERMENCİ<sup>1</sup>


<sup>1</sup>Kastamonu University, Faculty of Architecture and Engineering, Department of Environmental Engineering, 37150, Kastamonu, Türkiye


**Abstract:** In this study, the removal of moxifloxacin, an antibiotic of the fluoroquinolone group, from aqueous solutions was investigated using the electro-Fenton process. As the efficiency of the electro-Fenton process is highly dependent on the amount of H<sub>2</sub>O<sub>2</sub> produced during process, the formation of H<sub>2</sub>O<sub>2</sub> under acidic conditions was also investigated. In this context, the effects of applied current, cathode type and O<sub>2</sub> flow rate on H<sub>2</sub>O<sub>2</sub> production were investigated using boron-doped diamond anode. The highest H<sub>2</sub>O<sub>2</sub> production was achieved using the boron-doped diamond anode and the graphite felt cathode. In addition, the optimum conditions for the applied current and oxygen flow rate for H<sub>2</sub>O<sub>2</sub> production were determined to be 0.25 A and 0.1 L min<sup>-1</sup>, respectively. The effects of applied current and Fe<sup>2+</sup> concentration in the electro-Fenton process on the removal of moxifloxacin were investigated. It was found that the moxifloxacin removal rate increased with increasing applied current. The highest H<sub>2</sub>O<sub>2</sub> accumulation was observed at 0.25 A applied current, and moxifloxacin removal also reached 93.6% after 60 min. The moxifloxacin removal rate reached the highest value at Fe<sup>2+</sup> concentration of 0.01 mM. This study provides promising results for the efficient treatment of moxifloxacin-containing wastewater by the electro-Fenton process without the addition of H<sub>2</sub>O<sub>2</sub> using boron-doped diamond anode and graphite felt cathode.

**Keywords:** Electro-Fenton, Electro-generated H<sub>2</sub>O<sub>2</sub>, Moxifloxacin, Boron-doped diamond anode, Graphite felt cathode

\*Corresponding author: Kastamonu University, Faculty of Architecture and Engineering, Department of Environmental Engineering, 37150, Kastamonu, Türkiye

E mail: gdegermenci@kastamonu.edu.tr (G. D. DEĞERMENCİ)

Gökçe Didar DEĞERMENCİ  <https://orcid.org/0000-0002-4533-9273>

Nejdet DEĞERMENCİ  <https://orcid.org/0000-0003-3135-1471>

Received: March 31, 2024

Accepted: May 04, 2024

Published: May 15, 2024

Cite as: Değermenci GD, Değermenci N. 2024. Electrochemical hydrogen peroxide generation and removal of moxifloxacin by electro-Fenton process. BSJ Eng Sci, 7(3): 539-546.

### 1. Introduction

Antibiotics, which have a wide range of uses, are drugs used in the treatment of infectious diseases caused by microorganisms and improve the quality of life (Kovalakova et al., 2020; Phoon et al., 2020). Considerable quantities (30 to 90 %) of the antibiotics used to enter the waste stream together with their metabolic products without being metabolized in the body (Carvalho and Santos, 2016). It can be found in surface waters and groundwater due to the widespread use of antibiotics and their inadequate removal in conventional wastewater treatment plants (Kümmerer, 2009; Li et al., 2015; Ngigi et al., 2020; Anh et al., 2021). Therefore, the presence of antibiotics in the aquatic environment leads to a disturbance of flora and fauna and risks to human health (Tiwari et al., 2017). Moxifloxacin (MOX), a third-generation fluoroquinolone, belongs to a group of antimicrobial agents with a broad spectrum of activity and increasing consumption (Van Doorslaer et al., 2011). MOX is widely used against both gram-positive and gram-negative bacteria by inhibiting DNA activity and for the treatment of skin infections (Guay, 2006; Nguyen et al., 2023). However, due to its low biodegradability, it is constantly discharged into the

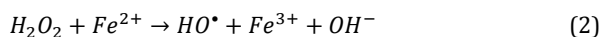
natural environment from conventional wastewater treatment plants (Van Doorslaer et al., 2015).

Antibiotics, which have high production and consumption rates, are not easily biodegradable. Therefore, cost-efficient methods are needed to effectively remove antibiotics from wastewater (Shoorangiz et al., 2019). As conventional treatment processes are not sufficient to remove wastewater containing antibiotics, advanced oxidation processes (AOPs) should be preferred to support them or be used as an alternative (Oturán and Aaron, 2014; Ganzenko et al., 2020; Taoufik et al., 2021). AOPs are methods of great interest for the removal of recalcitrant organics and toxic compounds (such as diclofenac and levofloxacin) (Jia et al., 2024; Qiu et al., 2024). AOPs such as Fenton, ozonation, photocatalysis, activated persulfate, and electrochemical processes have been used to remove toxic and/or recalcitrant organic pollutants (Değermenci et al., 2014; Çobanoğlu and Değermenci, 2022; Li et al., 2023). Among AOPs, Fenton oxidation attracts attention due to its simplicity, which does not require special equipment, and its high efficiency in removing organic pollutants (Arnold et al., 1995; Değermenci, 2023). To avoid disadvantages such as potential risks and loss of



reactive activity during transportation and storage of H<sub>2</sub>O<sub>2</sub> used in Fenton oxidation, the electro-Fenton process was developed in combination with Fe<sup>2+</sup> addition and in situ electro-generated H<sub>2</sub>O<sub>2</sub> (Zhou et al., 2007).

The electro-Fenton process is considered an environmentally friendly and promising method for the effective removal of target pollutants from water (Olvera-Vargas et al., 2021; Liu et al., 2022; Yang et al., 2023; de Oliveira Santiago Santos et al., 2023). In the electro-Fenton process, H<sub>2</sub>O<sub>2</sub> production is based on the electrochemical reduction of molecular oxygen (O<sub>2</sub>) at the cathode (Equation 1) by introducing air or high-purity O<sub>2</sub> into the electrolysis cell, and hydroxyl radicals are formed by the electrochemically assisted Fenton reaction (Equation 2) (Brillas et al., 2009). This process, hydrogen peroxide is continuously generated in situ, which allows better control of the oxidation process (Garcia-Segura et al., 2011; Bensalah et al., 2013). The hydroxyl radical and the hydrogen peroxide produced in the process have a strong oxidative potential (E<sub>0</sub>=2.80 V and 1.78 V) (Lucas and Peres, 2006). Non-selective hydroxyl radicals are responsible for the oxidation/mineralization of persistent organic substances that are in the same environment (Olvera-Vargas et al., 2021).



The performance of the electro-Fenton process depends largely on the electrode materials used during electrolysis (Guinea et al., 2010; Bensalah et al., 2013; Midassi et al., 2020). The type of cathode used influences the amount of H<sub>2</sub>O<sub>2</sub> produced by the reduction of molecular oxygen (Brillas et al., 2009; Olvera-Vargas et al., 2021). Materials such as carbon brush, carbon felt, stainless steel, carbon sponge etc. were used as cathodes (Sopaj et al., 2020; Olvera-Vargas et al., 2021). Although H<sub>2</sub>O<sub>2</sub> production in the electro-Fenton process depends on the cathode type, the structure of the anode material also plays an important role in the overall performance (Sopaj et al., 2016; Yang et al., 2020). Depending on the anode type, heterogeneous hydroxyl radicals are formed

on the anode surface by the oxidation of water (Titchou et al., 2021; Yang et al., 2023). The use of different types of anodes such as Pt, Ti/RuO<sub>2</sub>-IrO<sub>2</sub>, Ti<sub>4</sub>O<sub>7</sub>, boron doped diamond (BDD), and graphite felt (GF) in the electro-Fenton process has been investigated in the literature (Sopaj et al., 2016; Zwane et al., 2021). This increases the overall efficiency of the electro-Fenton process, as both the cathodic and anodic reactions contribute to the degradation/mineralization of the organic pollutants (Oturán et al., 2012; Olvera-Vargas et al., 2021). The BDD anode is characterized by a high O<sub>2</sub> evolution overvoltage (around 2.2 V vs SHE for BDD). BDD has proven to be the most effective material for the anodic oxidation of refractory organic pollutants (Panizza and Cerisola, 2009; Olvera-Vargas et al., 2021; Oturan, 2021), and the use of BDD as an anode in the electro-Fenton process has been shown to significantly improve the efficiency of the process (Oturán et al., 2012; Ridruejo et al., 2018; Olvera-Vargas et al., 2021).

In the first part of the study, the effects of different operating variables, such as cathode type, O<sub>2</sub> flow rate, and applied current on H<sub>2</sub>O<sub>2</sub> accumulation were discussed. In the second part, the removal of MOX by the electro-Fenton process using a BDD anode and a GF cathode was investigated. The effects of current intensity and Fe<sup>2+</sup> concentration, which are among the parameters affecting the electro-Fenton process, on MOX removal were investigated.

## 2. Materials and Methods

### 2.1. Chemicals

All chemicals and reagents used in this study were used without further purification. Moxifloxacin hydrochloride, potassium hydrogen phthalate, potassium iodide, sodium sulfate, hydrogen peroxide, ammonium heptamolybdate tetrahydrate, sodium hydroxide, and sulphuric acid were purchased from the Merck. All solutions were prepared with distilled water at room temperature.

### 2.2. Experimental Setup

A scheme of the electrochemical cell used is presented in Figure 1.

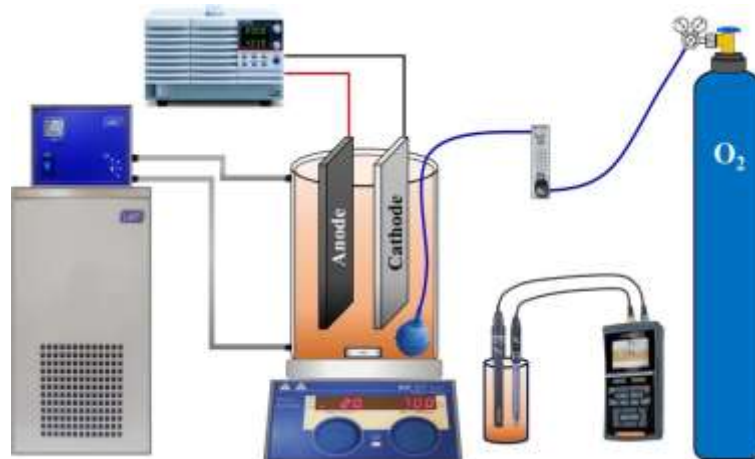


Figure 1. Schematic diagram of electrochemical cell.

Electrochemical  $\text{H}_2\text{O}_2$  production and MOX removal by the electro-Fenton process were carried out in an undivided cylindrical glass reactor with a diameter of 7.5 cm and a solution capacity of 400 mL. BDD electrode (DiaCCon GmbH, Germany) was used as an anode for  $\text{H}_2\text{O}_2$  production and the electro-Fenton process. GF, BDD, stainless steel (SS), and graphite plate (GP) electrodes were used as cathodes. All electrodes are 5 cm  $\times$  10 cm in size. The wall thickness is 3 mm for BDD, SS and GP and 12 mm for GF. The temperature of the solution was kept constant at 20°C using a temperature-controlled cooling/heated circulator (LABO, C200-H13). Sodium sulfate ( $\text{Na}_2\text{SO}_4$ ) was used as a supporting electrolyte to increase the conductivity of the solution. The aqueous solution was stirred continuously at 700 rpm with a magnetic stirrer (IKA, RCT basic). A power supply unit (GW Instek, PSW 80-40.5) was used in all experiments to ensure constant current operation. This device also displayed the cell voltage during the treatments. Without adding a buffer solution, the pH of the solution was adjusted to the desired value only once at the beginning of the experiment with 1 M  $\text{H}_2\text{SO}_4$ . The pH value of the solution was measured using the portable WTW Multi-Parameter meter (Xylem Analytics, MultiLine® Multi 3620 IDS).

### 2.3. Analytical Procedures

The  $\text{H}_2\text{O}_2$  and MOX concentration were measured using a UV-Vis spectrophotometer (HachLange, DR 6000). The  $\text{H}_2\text{O}_2$  concentration was measured at 352 nm by the iodometric method (Klassen et al., 1994). To measure the MOX concentration, a MOX stock solution was prepared and known MOX concentrations were determined by dilution. These solutions were used to create a calibration curve at 290 nm, and the unknown MOX concentrations were measured by prepared calibration curve. The MOX removal efficiency and energy consumption were calculated using Equation 3 and Equation 4, respectively:

$$\text{MOX removal, (\%)} = (1 - C_t/C_0) \times 100 \quad (3)$$

$$W, (\text{kWh m}^{-3}) = V \times I \times t/V_S \quad (4)$$

where  $C_0$  is the initial MOX concentration ( $\text{mg L}^{-1}$ ),  $C_t$  is the MOX concentration at given time  $t$  ( $\text{mg L}^{-1}$ ),  $V$  is mean cell voltage (V),  $I$  is electrolysis current (A),  $t$  is electrolysis duration (h), and  $V_S$  is solution volume (L).

## 3. Results and Discussion

### 3.1. Electrochemical $\text{H}_2\text{O}_2$ Production

The reactant required for the Fenton reaction to form strong oxidative free radicals is  $\text{H}_2\text{O}_2$  (Değermenci et al., 2019). The efficiency of the electro-Fenton process depends largely on the amount of  $\text{H}_2\text{O}_2$  produced in the system (Zhao et al., 2018). In the electro-Fenton process,  $\text{H}_2\text{O}_2$  can be formed under acidic conditions by the electrochemical reduction of oxygen at the cathode (Equation 1) (Brillas et al., 2009; Midassi et al., 2020). In this context, the effects of current intensity, cathode type,

and  $\text{O}_2$  flow rate, which are among the parameters affecting electrochemical  $\text{H}_2\text{O}_2$  production, were examined using the BDD anode.

#### 3.1.1. Effect of cathode type on $\text{H}_2\text{O}_2$ production

$\text{H}_2\text{O}_2$  production varies depending on the cathode material (Oturan et al., 2021). Therefore, the  $\text{H}_2\text{O}_2$  production performance of different cathode types using BDD as anode material was investigated.  $\text{H}_2\text{O}_2$  formation in the experimental system was measured in a solution saturated with  $\text{O}_2$  under acidic conditions ( $\text{pH} = 3$ ) and in the absence of pollutants and  $\text{Fe}^{2+}$ .  $\text{H}_2\text{O}_2$  production was monitored for 60 min by continuously supplying  $\text{O}_2$  to the cathode; the results are shown in Figure 2. The  $\text{H}_2\text{O}_2$  production during 60 min electrolysis is 42.7, 28.1, 15.4, and 11.1  $\text{mg L}^{-1}$  for GF, BDD, SS, and GP, respectively. The highest  $\text{H}_2\text{O}_2$  production was achieved with GF. The  $\text{H}_2\text{O}_2$  production during 30 min electrolysis is 36.4, 20, 14.1 and 10.0  $\text{mg L}^{-1}$  for GF, BDD, SS and GP, respectively. These results show that the  $\text{H}_2\text{O}_2$  production rate depends significantly on the cathode type. However, it can be said that the electrochemical reduction of molecular oxygen (Equation 1) occurs faster when GF is used as the cathode. The type of cathode promotes oxygen adsorption and transfer, electron transfer and provides more active sites, thereby promoting the production of  $\text{H}_2\text{O}_2$  (Feng et al., 2021). Since the highest  $\text{H}_2\text{O}_2$  production was obtained with GF, it was used as the cathode in the following studies.

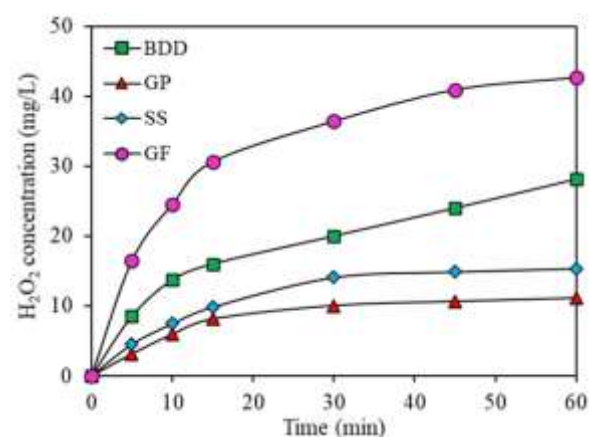


**Figure 2.** Effect of cathode type on the  $\text{H}_2\text{O}_2$  generation (Conditions: Current intensity= 1 A,  $\text{Na}_2\text{SO}_4$ = 50 mM,  $T$ = 20°C, initial solution  $\text{pH} = 3$ , and  $\text{O}_2$  flow rate= 1  $\text{L min}^{-1}$ ).

#### 3.1.2. Effect of applied current on $\text{H}_2\text{O}_2$ production

The applied current is one of the most important parameters for electrochemical  $\text{H}_2\text{O}_2$  production (Köktaş and Gökkuş, 2022). The cathodic production of  $\text{H}_2\text{O}_2$  via the reaction given in Equation 1 drives the production of hydroxyl radicals in the electro-Fenton process via the reaction given in Equation 2. Therefore, the  $\text{H}_2\text{O}_2$  accumulation in the electrolysis reactor with BDD anode and GF cathode was investigated. Figure 3 shows the  $\text{H}_2\text{O}_2$  accumulation at different current values during the 60 min electrolysis at an initial solution  $\text{pH}$  of 3, an electrolyte concentration of 50 mM  $\text{Na}_2\text{SO}_4$  and an

oxygen flow rate of  $1 \text{ L min}^{-1}$ . The  $\text{H}_2\text{O}_2$  concentration is  $23.6 \text{ mg L}^{-1}$  after 60 min of electrolysis at a current of 0.05 A. When the current was raised from 0.10 to 0.25 A, the  $\text{H}_2\text{O}_2$  concentration increased from 53.8 to  $95.7 \text{ mg L}^{-1}$ . The reason for this increase is that an increase in the applied current supports the oxygen reduction reaction specified in equation 1. However, a further increase in the applied current led to a decrease in  $\text{H}_2\text{O}_2$  accumulation.  $\text{H}_2\text{O}_2$  concentration decreased from 66.8 to  $42.7 \text{ mg L}^{-1}$  when the current was increased from 0.50 to 1.00 A, respectively. This is because the competitive reactions increase with increasing applied current, which leads to a depletion of  $\text{H}_2\text{O}_2$ . These are explained by the reduction of  $\text{H}_2\text{O}_2$  to  $\text{H}_2\text{O}$  at the cathode (Equation 5) and the oxidation of  $\text{H}_2\text{O}_2$  at the anode (Equation 6). Similar results have been reported regarding the effect of applied current on  $\text{H}_2\text{O}_2$  production (Zhou et al., 2019; Midassi et al., 2020; Olvera-Vargas et al., 2021). Subsequent experiments were carried out at 0.10 A in order to determine the effect of other operating parameters and for cost effectiveness.

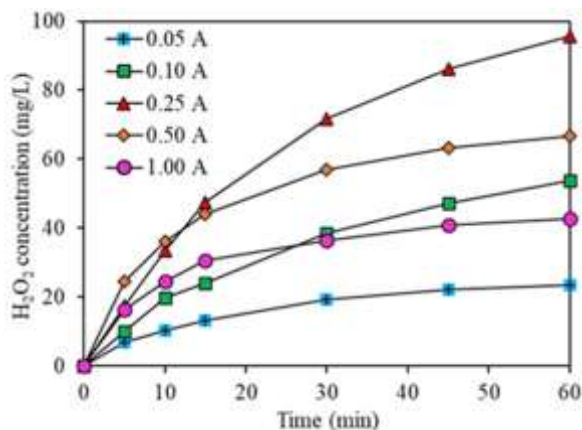
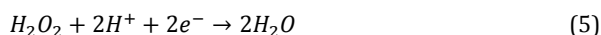


**Figure 3.** Effect of applied current on the  $\text{H}_2\text{O}_2$  generation (Conditions:  $\text{Na}_2\text{SO}_4 = 50 \text{ mM}$ ,  $T = 20^\circ\text{C}$ , initial solution  $\text{pH} = 3$ , and  $\text{O}_2$  flow rate =  $1 \text{ L min}^{-1}$ ).

### 3.1.3. Effect of $\text{O}_2$ flow rate on $\text{H}_2\text{O}_2$ production

The  $\text{O}_2$  flow rate supplied to the system is one of the parameters that influence electrochemical  $\text{H}_2\text{O}_2$  production (Midassi et al., 2020). Figure 4 shows the effects of  $\text{O}_2$  flow rate on  $\text{H}_2\text{O}_2$  production when using a BDD anode and a GF cathode. In the experiments, the effect of different  $\text{O}_2$  flow rates ( $0\text{--}1 \text{ L min}^{-1}$ ) on  $\text{H}_2\text{O}_2$  production was studied for electrolysis time of 60 min. While  $\text{H}_2\text{O}_2$  production is  $14.9 \text{ mg L}^{-1}$  when no gas is added to the reactor,  $\text{H}_2\text{O}_2$  production increases when  $\text{O}_2$  is introduced. At an  $\text{O}_2$  flow rate of  $0.1 \text{ L min}^{-1}$ ,  $\text{H}_2\text{O}_2$  accumulation reached the highest value of  $61.3 \text{ mg L}^{-1}$  in 60 min. A further increase in the gas flow rate reduced  $\text{H}_2\text{O}_2$  production to  $53.9 \text{ mg L}^{-1}$  at  $0.2 \text{ L min}^{-1}$  and  $53.8 \text{ mg L}^{-1}$  at  $1.0 \text{ L min}^{-1}$ . Increasing the  $\text{O}_2$  flow rate can

increase the concentration of dissolved  $\text{O}_2$  and promote the mass transfer rate of dissolved  $\text{O}_2$  in the solution, which supports electro-generated  $\text{H}_2\text{O}_2$  production. At flow rates greater than  $0.1 \text{ L min}^{-1}$ , excessively large bubbles covering the surface of the gas diffusion electrode lead to reduced  $\text{H}_2\text{O}_2$  production. Similar results regarding the effect of  $\text{O}_2$  flow rate on  $\text{H}_2\text{O}_2$  production have been reported in some studies (Xia et al., 2019; Köktaş and Gökkuş, 2022). A flow rate of  $0.1 \text{ L min}^{-1}$   $\text{O}_2$  is sufficient to generate a high  $\text{H}_2\text{O}_2$  concentration. These results show that adjusting the optimal  $\text{O}_2$  flow rate in the system can not only promote  $\text{H}_2\text{O}_2$  production but also reduce costs (Zhou et al., 2013).

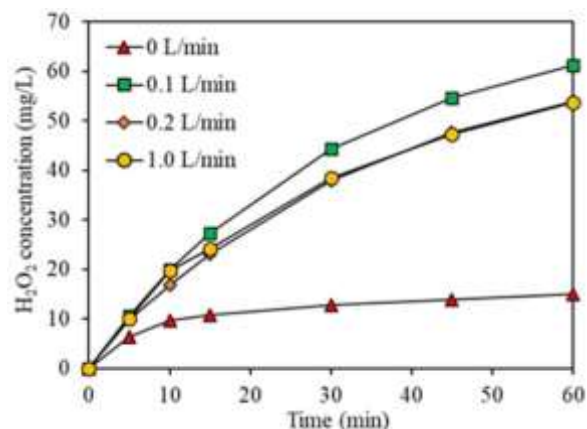


**Figure 4.** Effect of the  $\text{O}_2$  flow rate on the  $\text{H}_2\text{O}_2$  generation (Conditions:  $\text{Na}_2\text{SO}_4 = 50 \text{ mM}$ ,  $T = 20^\circ\text{C}$ , initial solution  $\text{pH} = 3$ , and current intensity =  $0.10 \text{ A}$ ).

### 3.2. Effect of Different Processes on MOX Removal

In the system in which the highest  $\text{H}_2\text{O}_2$  production was achieved, graphite felt was used as the cathode and BDD as the anode. In the electrolytic cell, MOX can be removed by adsorption and anodic oxidation together with the electro-Fenton process. A comparison of the MOX removals achieved with these treatment methods is shown in Figure 5. In the experiment to determine the amount of MOX adsorbed on the anode and cathode in the electrolytic cell, no current was applied to the cell and  $\text{O}_2$  and  $\text{Fe}^{2+}$  were not supplied. It was determined that the removal of MOX by adsorption was 11.7% in 10 min and 27.5% in 60 min. Then the removal of MOX by anodic oxidation was determined by applying current ( $0.10 \text{ A}$ ) to the electrolytic cell without  $\text{O}_2$  and  $\text{Fe}^{2+}$ . While MOX removal by anodic oxidation was 30.9% at the 10 min electrolysis, it increased to 87.7% after 60 min. Finally, MOX removal was determined by the electro-Fenton process by adding  $\text{O}_2$  and  $\text{Fe}^{2+}$  to the electrolytic cell at a certain current value ( $0.10 \text{ A}$ ). MOX removal by the electro-Fenton process increased from 67.3% in 10 min to 89.0% after 60 min. From these results, it was concluded that the electro-Fenton process is the treatment process with the highest removal rate.

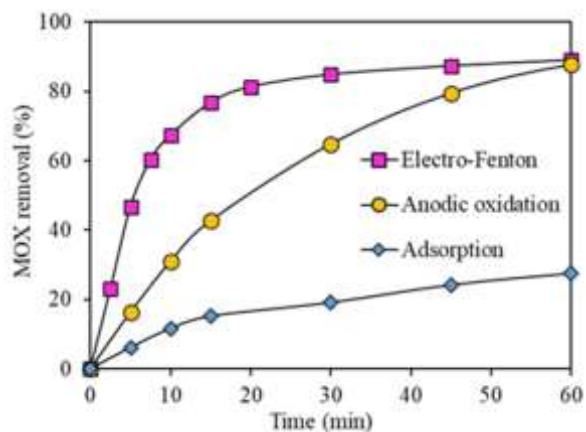


**Figure 5.** Comparison between electro-Fenton, anodic oxidation and adsorption (Conditions: MOX= 5 mg L<sup>-1</sup>, Na<sub>2</sub>SO<sub>4</sub>= 50 mM, initial solution pH= 3, T= 20°C, current intensity= 0.10 A, O<sub>2</sub> flow rate= 0.1 L min<sup>-1</sup>, Fe<sup>2+</sup>= 0.01mM).

### 3.2.1. Effect of applied current on MOX removal in the electro-Fenton process

The applied current considerably influences on the electro-Fenton process and is the most important parameter for controlling the reaction rate (Görmez et al., 2022). The effect of the applied current on the removal of MOX by the electro-Fenton process using a GF cathode and a BDD anode is shown in Figure 6. In the electro-Fenton process, MOX removal efficiencies at 60 min electrolysis time were 86.4%, 89.0%, 93.6%, 95.2% and 95.6% at applied currents of 0.05, 0.10, 0.25, 0.50 and 0.75 A, respectively. During the 10 min electrolysis time, MOX removal was 59.6%, 67.3%, 78.5%, 84.6% and 88.5%, respectively, depending on the increasing current value applied. From these results, it can be concluded that the MOX removal rate increases with the increase of the applied current. Comparing these results with H<sub>2</sub>O<sub>2</sub> production, the highest H<sub>2</sub>O<sub>2</sub> accumulation was obtained at 0.25 A (Figure 3), which does not correspond to the optimum current value for MOX removal. The decreasing H<sub>2</sub>O<sub>2</sub> accumulation at high current values does not mean that H<sub>2</sub>O<sub>2</sub> production is low. It means that the rate of competitive reactions (Equations 5 and 6) leading to H<sub>2</sub>O<sub>2</sub> depletion is high, so the rate of H<sub>2</sub>O<sub>2</sub> decomposition is faster than the formation of H<sub>2</sub>O<sub>2</sub> (Olvera-Vargas et al., 2021). The H<sub>2</sub>O<sub>2</sub> produced in the electrolytic cell reacted with Fe<sup>2+</sup> via the Fenton reaction (equation 2) before being destroyed via equations 5 and 6. It should be noted that increasing the applied current value increases electrical energy consumption and operating costs.

The change in energy consumption in the experiments conducted at different current values was calculated using equation 4, and the results are shown in Figure 7. As the current value applied to the system increases, the energy consumption increases along with the increase in voltage. The energy consumption for currents of 0.05, 0.10, 0.25, 0.50 and 0.75 A was calculated to be 0.38, 0.86, 2.53, 6.59 and 12.0 kWh m<sup>-3</sup>, at the end of 60 min,

respectively. Increasing the applied current can lead to chemical changes on the electrode surface and shorten the service life of the electrode (GilPavas et al., 2017). However, a further increase in the applied current can have a negative effect on MOX removal due to side reactions (hydrogen evolution and water electrolysis) (Qiu et al., 2024).

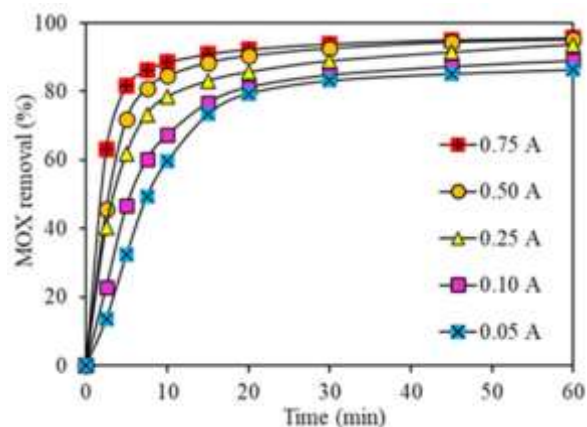


**Figure 6.** Effect of applied current on the MOX removal in the electro-Fenton process (Conditions: MOX= 5 mg L<sup>-1</sup>, Na<sub>2</sub>SO<sub>4</sub>= 50 mM, initial solution pH= 3, T= 20°C, O<sub>2</sub> flow rate= 0.1 L min<sup>-1</sup>, Fe<sup>2+</sup>= 0.01mM).

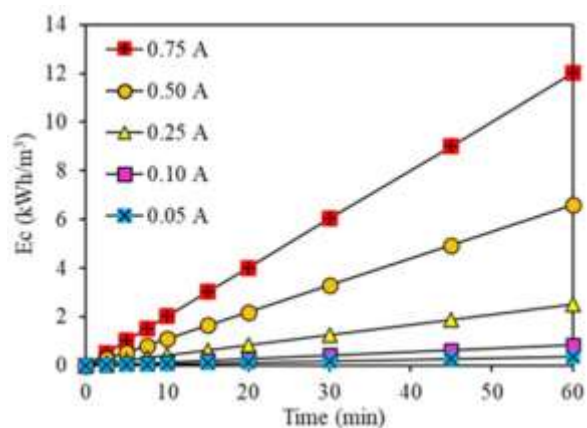


**Figure 7.** Variation of energy consumption with applied current (Conditions: MOX= 5 mg L<sup>-1</sup>, Na<sub>2</sub>SO<sub>4</sub>= 50 mM, initial solution pH= 3, T= 20°C, O<sub>2</sub> flow rate= 0.1 L min<sup>-1</sup>, Fe<sup>2+</sup>= 0.01mM).

### 3.2.2. Effect of Fe<sup>2+</sup> concentration on MOX removal in the electro-Fenton process

The catalyst concentration is one of the important parameters affecting the removal of pollutants in the electro-Fenton process (Wang et al., 2021; Karatas et al., 2022). The effect of Fe<sup>2+</sup> concentration on MOX removal is shown in Figure 8. While in the absence of Fe<sup>2+</sup> ions the MOX removal in 10 min was about 30.9 %, a significant increase in MOX removal was observed with the addition of Fe<sup>2+</sup> ions. At an electrolysis time of 10 min, the Fe<sup>2+</sup> concentration for MOX removal increased to 63.4 % at 0.005 mM and to 67.3 % at 0.010 mM. This increase in MOX removal can be explained by the contribution of the generated hydroxyl radicals (Equation 2). Increasing the

Fe<sup>2+</sup> concentration to 0.020 mM led to a slight decrease in MOX removal. This negative effect of the high Fe<sup>2+</sup> concentration can be explained by the increased rate of the parasitic reaction (Equation 7) that occurs between hydroxyl radicals and excess Fe<sup>2+</sup> (Özdemir et al., 2011; Xia et al., 2019).

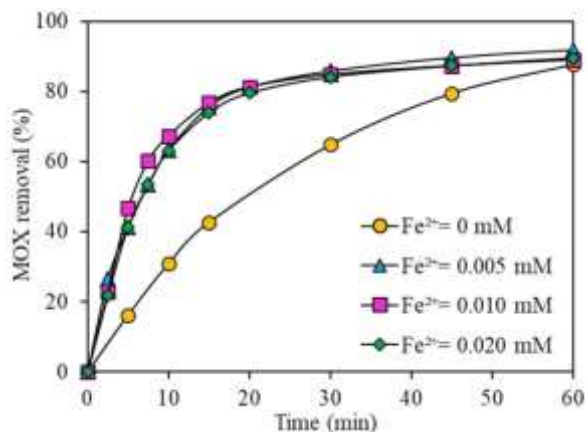


**Figure 8.** Effect of Fe<sup>2+</sup> concentration on MOX removal in the electro-Fenton process (Conditions: MOX= 5 mg L<sup>-1</sup>, Na<sub>2</sub>SO<sub>4</sub>= 50 mM, initial solution pH= 3, T= 20°C, current intensity= 0.10 A, O<sub>2</sub> flow rate= 0.1 L min<sup>-1</sup>).

#### 4. Conclusion

In this study, electrochemical H<sub>2</sub>O<sub>2</sub> production and MOX removal were successfully performed with a BDD anode. It was found that the electrochemical H<sub>2</sub>O<sub>2</sub> production rate was significantly dependent on the cathode type. H<sub>2</sub>O<sub>2</sub> production increased with the use of a GF cathode, it was also observed that the applied current and oxygen flow rate also had significant effects on H<sub>2</sub>O<sub>2</sub> production. The effects of applied current and Fe<sup>2+</sup> concentration on MOX removal in the electro-Fenton process were investigated. It was found that the MOX removal rate in the process with BDD anode and GF cathode increased with the increase of the applied current. However, it was found that increasing current was accompanied by a corresponding increase in energy consumption due to the increased voltage. From the findings, it was concluded that the electro-Fenton process could be an effective method for reducing antibiotic contamination in wastewater.

#### Author Contributions

The percentage of the author(s) contributions is presented below. The author reviewed and approved the final version of the manuscript.

	G.D.D.	N.D.
C	70	30
D	70	30
S	100	
DCP	50	50
DAI	50	50
L	80	20
W	100	
CR	80	20
SR	100	
PM	80	20
FA	100	

C=Concept, D= design, S= supervision, DCP= data collection and/or processing, DAI= data analysis and/or interpretation, L= literature search, W= writing, CR= critical review, SR= submission and revision, PM= project management, FA= funding acquisition.

#### Conflict of Interest

The author declared that there is no conflict of interest.

#### Ethical Consideration

Ethics committee approval was not required for this study because of there was no study on animals or humans.

#### Acknowledgements

This research has been supported by Kastamonu University Scientific Research Projects Coordination Department (Project Number: KÜ-BAP01/2018-97).

#### References

- Anh HQ, Le TPQ, Le ND, Lu XX, Duong TT, Garnier J, Rochelle-Newall E, Zhang S, Oh N-H, Oeurng C, Ekkawatpanit C, Nguyen TD, Nguyen QT, Nguyen TD, Nguyen TN, Tran TL, Kunisue T, Tanoue R, Takahashi S, Minh TB, Le TL, Pham TNM, Nguyen TAH. 2021. Antibiotics in surface water of East and Southeast Asian countries: A focused review on contamination status, pollution sources, potential risks, and future perspectives. *Sci Total Environ*, 764: 142865.
- Arnold SM, Hickey WJ, Harris RF. 1995. Degradation of atrazine by Fenton's reagent: Condition optimization and product quantification. *Environ Sci Technol*, 29: 2083-2089.
- Bensalah N, Bedoui A, Chellam S, Abdel-Wahab A. 2013. Electro-Fenton treatment of photographic processing wastewater. *Clean (Weinh)*, 41: 635-644.
- Brillas E, Sirés I, Oturan MA. 2009. Electro-fenton process and related electrochemical technologies based on fenton's reaction chemistry. *Chem Rev*, 109: 6570-6631.
- Carvalho IT, Santos L. 2016. Antibiotics in the aquatic environments: A review of the European scenario. *Environ Int*, 94: 736-757.
- Çobanoğlu K, Değermenci N. 2022. Comparison of reactive azo dye removal with UV/H<sub>2</sub>O<sub>2</sub>, UV/S<sub>2</sub>O<sub>8</sub><sup>2-</sup> and UV/H<sub>2</sub>O<sub>2</sub>/S<sub>2</sub>O<sub>8</sub><sup>2-</sup> processes in aqueous solutions. *Environ Monit Assess*, 194: 302.

- De Oliveira Santiago Santos G, Athie Goulart L, Sánchez-Montes I, Da Silva RS, De Vasconcelos Lanza MR. 2023. Electrochemically enhanced iron oxide-modified carbon cathode toward improved heterogeneous electro-Fenton reaction for the degradation of norfloxacin. *Environ Sci Pollut Res Int*, 30: 118736-118753.
- Değermenci GD, Bayhan YK, Değermenci N. 2014. Investigation of treatability of industrial wastewater containing high organic matter by Fenton process. *J Inst Sci Technol*, 4(2): 17-22.
- Değermenci GD. 2023. Decolorization of reactive azo dye by fenton and photo-fenton processes in aqueous solution: The influence of operating conditions, kinetics study, and performance comparison. *Bull Chem Soc Ethiop*, 37: 197-210.
- Değermenci N, Değermenci GD, Ulu HB. 2019. Decolorization of reactive azo dye from aqueous solutions with Fenton oxidation process: effect of system parameters and kinetic study. *Desalin Water Treat*, 169: 363-371.
- Feng Y, Li W, An J, Zhao Q, Wang X, Liu J, He W, Li N. 2021. Graphene family for hydrogen peroxide production in electrochemical system. *Sci Total Environ*, 769: 144491.
- Ganzenko O, Trelu C, Oturan N, Huguenot D, Péchaud Y, Van Hullebusch ED, Oturan MA. 2020. Electro-Fenton treatment of a complex pharmaceutical mixture: Mineralization efficiency and biodegradability enhancement. *Chemosphere*, 253: 126659.
- Garcia-Segura S, Centellas F, Arias C, Garrido JA, Rodríguez RM, Cabot PL, Brillas E. 2011. Comparative decolorization of monoazo, diazo and triazo dyes by electro-Fenton process. *Electrochim Acta*, 58: 303-311.
- GilPavas E, Arbeláez-Castaño P, Medina J, Acosta DA. 2017. Combined electrocoagulation and electro-oxidation of industrial textile wastewater treatment in a continuous multi-stage reactor. *Water Sci Technol*, 76: 2515-2525.
- Görmez Ö, Akay S, Gözmen B, Kayan B, Kaldersı D. 2022. Degradation of emerging contaminant coumarin based on anodic oxidation, electro-Fenton and subcritical water oxidation processes. *Environ Res*, 208: 112736.
- Guay DRP. 2006. Moxifloxacin in the treatment of skin and skin structure infections. *Ther Clin Risk Manag*, 2: 417-434.
- Guinea E, Garrido JA, Rodríguez RM, Cabot P-L, Arias C, Centellas F, Brillas E. 2010. Degradation of the fluoroquinolone enrofloxacin by electrochemical advanced oxidation processes based on hydrogen peroxide electrogeneration. *Electrochim Acta*, 55: 2101-2115.
- Jia X, Huang J, Zhao X, Wu T, Wang C, He H. 2024. Levofloxacin degradation in a heterogeneous electro-Fenton system with an FeOCl/MoS<sub>2</sub> composite catalyst. *React Chem Eng*, 9: 1127-1139. <https://doi.org/10.1039/d3re00548h>.
- Karatas O, Gengec NA, Gengec E, Khataee A, Kobya M. 2022. High-performance carbon black electrode for oxygen reduction reaction and oxidation of atrazine by electro-Fenton process. *Chemosphere*, 287: 132370.
- Klassen N V, Marchington D, McGowan HCE. 1994. H<sub>2</sub>O<sub>2</sub> Determination by the I<sub>3</sub>- Method and by KMnO<sub>4</sub> Titration. *Anal Chem*, 66: 2921-2925.
- Köktaş İY, Gökkuş Ö. 2022. Removal of salicylic acid by electrochemical processes using stainless steel and platinum anodes. *Chemosphere*, 293: 133566.
- Kovalakova P, Cizmas L, McDonald TJ, Marsalek B, Feng M, Sharma VK. 2020. Occurrence and toxicity of antibiotics in the aquatic environment: A review. *Chemosphere*, 251: 126351.
- Kümmerer K. 2009. Antibiotics in the aquatic environment - A review - Part I. *Chemosphere*, 75: 417-434.
- Li S, Wu Y, Zheng H, Li H, Zheng Y, Nan J, Ma J, Nagarajan D, Chang J-S. 2023. Antibiotics degradation by advanced oxidation process (AOPs): Recent advances in ecotoxicity and antibiotic-resistance genes induction of degradation products. *Chemosphere*, 311: 136977.
- Li W, Gao L, Shi Y, Liu J, Cai Y. 2015. Occurrence, distribution and risks of antibiotics in urban surface water in Beijing, China. *Environ Sci Process Impacts*, 17: 1611-1619.
- Liu Z-j, Wan J-q, Yan Z-c, Wang Y, Ma Y-w. 2022. Efficient removal of ciprofloxacin by heterogeneous electro-Fenton using natural air-cathode. *Chem Eng J*, 433: 133767.
- Lucas MS, Peres JA. 2006. Decolorization of the azo dye Reactive Black 5 by Fenton and photo-Fenton oxidation. *Dye Pigment*, 71: 236-244.
- Midassi S, Bedoui A, Bensalah N. 2020. Efficient degradation of chloroquine drug by electro-Fenton oxidation: Effects of operating conditions and degradation mechanism. *Chemosphere*, 260: 127558.
- Ngigi AN, Magu MM, Muendo BM. 2020. Occurrence of antibiotics residues in hospital wastewater, wastewater treatment plant, and in surface water in Nairobi County, Kenya. *Environ Monit Assess*, 192: 18.
- Nguyen TH, Nguyen XH, Do TG, Nguyen LH. 2023. Development of biochar supported NiFe<sub>2</sub>O<sub>4</sub> composite for peroxydisulfate (PDS) activation to effectively remove moxifloxacin from wastewater. *Chem Eng J Adv*, 16: 100550.
- Olvera-Vargas H, Gore-Datar N, Garcia-Rodriguez O, Mutnuri S, Lefebvre O. 2021. Electro-Fenton treatment of real pharmaceutical wastewater paired with a BDD anode: Reaction mechanisms and respective contribution of homogeneous and heterogeneous OH. *Chem Eng J*, 404: 126524.
- Oturan MA, Aaron JJ. 2014. Advanced oxidation processes in water/wastewater treatment: Principles and applications. A review. *Crit Rev Environ Sci Technol*, 44: 2577-2641.
- Oturan MA. 2021. Outstanding performances of the BDD film anode in electro-Fenton process: Applications and comparative performance. *Curr Opin Solid State Mater Sci*, 25: 100925.
- Oturan N, Bo J, Trelu C, Oturan MA. 2021. Comparative Performance of Ten Electrodes in Electro-Fenton Process for Removal of Organic Pollutants from Water. *ChemElectroChem*, 8: 3294-3303.
- Oturan N, Brillas E, Oturan MA. 2012. Unprecedented total mineralization of atrazine and cyanuric acid by anodic oxidation and electro-Fenton with a boron-doped diamond anode. *Environ Chem Lett*, 10: 165-170.
- Özdemir C, Öden MK, Şahinkaya S, Kalipçi E. 2011. Color Removal from Synthetic Textile Wastewater by Sono-Fenton Process. *Clean (Weinh)*, 39: 60-67.
- Panizza M, Cerisola G. 2009. Direct and mediated anodic oxidation of organic pollutants. *Chem Rev*, 109: 6541-6569.
- Phoon BL, Ong CC, Mohamed Saheed MS, Show P-L, Chang J-S, Ling TC, Lam SS, Juan JC. 2020. Conventional and emerging technologies for removal of antibiotics from wastewater. *J Hazard Mater*, 400: 122961.
- Qiu B, Zhou X, Li W, Hhu H, Yu L, Yuan C, Dou R, Sun M, Wang S. 2024. A magnetically induced self-assembly of Ru@Fe<sub>3</sub>O<sub>4</sub>/rGO cathode for diclofenac degradation in electro-Fenton process. *Environ Res*, 242: 117781.
- Ridruejo C, Centellas F, Cabot PL, Sirés I, Brillas E. 2018. Electrochemical Fenton-based treatment of tetracaine in synthetic and urban wastewater using active and non-active anodes. *Water Res*, 128: 71-81.
- Shoorangiz M, Nikoo MR, Salari M, Rakhshandehroo GR, Sadegh

- M. 2019. Optimized electro-Fenton process with sacrificial stainless steel anode for degradation/mineralization of ciprofloxacin. *Process Saf Environ Prot*, 132: 340-350.
- Sopaj F, Oturan N, Pinson J, Podvorica F, Oturan MA. 2016. Effect of the anode materials on the efficiency of the electro-Fenton process for the mineralization of the antibiotic sulfamethazine. *Appl Catal B Environ*, 199: 331-341.
- Sopaj F, Oturan N, Pinson J, Podvorica FI, Oturan MA. 2020. Effect of cathode material on electro-Fenton process efficiency for electrocatalytic mineralization of the antibiotic sulfamethazine. *Chem Eng J*, 384: 123249.
- Taoufik N, Boumya W, Achak M, Sillanpää M, Barka N. 2021. Comparative overview of advanced oxidation processes and biological approaches for the removal pharmaceuticals. *J Environ Manage*, 288: 112404.
- Titchou FE, Zazou H, Afanga H, Gaayda JE, Akbour RA, Hamdani M, Oturan MA. 2021. Electro-Fenton process for the removal of Direct Red 23 using BDD anode in chloride and sulfate media. *J Electroanal Chem*, 897: 115560.
- Tiwari B, Sellamuthu B, Ouarda Y, Drogui P, Tyagi RD, Buelna G. 2017. Review on fate and mechanism of removal of pharmaceutical pollutants from wastewater using biological approach. *Bioresour Technol*, 224: 1-12.
- Van Doorslaer X, Demeestere K, Heynderickx PM, Van Langenhove H, Dewulf J. 2011. UV-A and UV-C induced photolytic and photocatalytic degradation of aqueous ciprofloxacin and moxifloxacin: Reaction kinetics and role of adsorption. *Appl Catal B Environ*, 101: 540-547.
- Van Doorslaer X, Dewulf J, De Maerschalk J, Van Langenhove H, Demeestere D. 2015. Heterogeneous photocatalysis of moxifloxacin in hospital effluent: Effect of selected matrix constituents. *Chem Eng J*, 261: 9-16.
- Wang Y, Chen J, Gao J, Meng H, Chai S, Jian Y, Shi L, Wang Y, He C. 2021. Selective electrochemical H<sub>2</sub>O<sub>2</sub> generation on the graphene aerogel for efficient electro-Fenton degradation of ciprofloxacin. *Sep Purif Technol*, 272: 118884.
- Xia Y, Shang H, Zhang Q, Zhou Y, Hu X. 2019. Electrogeneration of hydrogen peroxide using phosphorus-doped carbon nanotubes gas diffusion electrodes and its application in electro-Fenton. *J Electroanal Chem*, 840: 400-408.
- Yang W, Oturan N, Liang J, Oturan MA. 2023. Synergistic mineralization of ofloxacin in electro-Fenton process with BDD anode: Reactivity and mechanism. *Sep Purif Technol*, 319: 124039.
- Yang W, Oturan N, Raffy S, Zhou M, Oturan MA. 2020. Electrocatalytic generation of homogeneous and heterogeneous hydroxyl radicals for cold mineralization of anti-cancer drug Imatinib. *Chem Eng J*, 383: 123155.
- Zhao K, Quan X, Chen S, Yu H, Zhang Y, Zhao H. 2018. Enhanced electro-Fenton performance by fluorine-doped porous carbon for removal of organic pollutants in wastewater. *Chem Eng J*, 354: 606-615.
- Zhou L, Hu Z, Zhang C, Bi Z, Jin T, Zhou M. 2013. Electrogeneration of hydrogen peroxide for electro-Fenton system by oxygen reduction using chemically modified graphite felt cathode. *Sep Purif Technol*, 111: 131-136.
- Zhou M, Yu Q, Lei L, Barton G. 2007. Electro-Fenton method for the removal of methyl red in an efficient electrochemical system. *Sep Purif Technol*, 57: 380-387.
- Zhou W, Rajic L, Meng X, Nazari R, Zhao Y, Wang Y, Gao J, Qin Y, Alshwabkeh AN. 2019. Efficient H<sub>2</sub>O<sub>2</sub> electrogeneration at graphite felt modified via electrode polarity reversal: Utilization for organic pollutants degradation. *Chem Eng J*, 364: 428-439.
- Zwane BN, Orimolade BO, Koiki BA, Mabuba N, Gomri C, Petit E, Bonniol V, Lesage G, Rivallin M, Cretin M, Arotiba OA. 2021. Combined electro-fenton and anodic oxidation processes at a sub-stoichiometric titanium oxide (Ti<sub>4</sub>O<sub>7</sub>) ceramic electrode for the degradation of tetracycline in water. *Water (Basel)*, 13: 2772.